DEMONSTRATION OF SOLAR-PUMPED LASER-INDUCED MAGNESIUM PRODUCTION FORM MAGNESIUM OXIDE

Yabe Takashi; Ohkubo Tomomasa; Dinh Thanh Hung; Kuboyama Hiroki; Nakano Junichi; Okamoto Kouta;
Tokyo Institute of Technology, 2-12-1 O-okayama, Meguro-ku, Tokyo 152-8550, Japan

Keywords: Laser-induced magnesium production, solar-pumped laser, fossil-fuel-free energy cycle.

Abstract

Studies of storing solar energy into chemical energy of magnesium (Mg) through reduction from magnesium oxide (MgO) by solar-pumped laser were conducted. We succeeded in solar-pumped laser-induced Mg production. Laser system consists of a 4 m^2 Fresnel lens mounting on a sun tracker platform which focus solar radiation into laser head therefore over 100W (CW) output laser can be irradiated. A single laser beam is focused on a mixture of magnesium oxide and reducing agent silicon. High power density of focused laser leads to high temperature and the reduction reaction resulting in Mg production. The resultant vapor is collected on a copper plate and analyzed in terms of magnesium deposition efficiency. As a result, deposition efficiency of 2.3 mg/kJ was achieved.

Introduction

More than 80% of the world total primary energy is provided by fossil fuel that otherwise emit greenhouse gases causing global warming. World demand for energy would be more than doubled by year 2050 and more than tripled by the end of century. Current improvements in existing energy networks will not be adequate for this demand in a sustainable way. Finding sufficient supplies of renewable energy for future is one of the challenges that scientist face. There is no doubt that solar energy is an ultimate renewable energy source, however, it is only available in the clear daytime and therefore, needs a reliable storing means as main energy source in future.

Authors proposed to use the chemical potential of magnesium as solar energy reservoir. Magnesium was chosen because it is the eighth most abundant element in the earth's crust (although it cannot be found in its elemental form in nature). It is also the second richest metal element in seawater with concentration of 1.3 g/l. In addition, magnesium is relatively light metal suitable for transportation and has a large energy storage capacity of 43 GJ/m^3 compared to 4.3 GJ/m^3 of hydrogen stored at 70MPa. Magnesium reacts with steam to generate hydrogen and release 359.8 kJ/mol of thermal energy as follows:

$$Mg_{(s)} + H_2O_{(s)} \rightarrow MgO_{(s)} + H_{2(g)}, \quad \Delta H = -359.8 \text{ kJ/mol.}$$
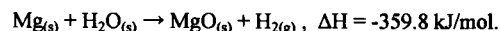
Hydrogen generated further react with oxygen to give steam and additional energy.

$$H_{2(g)} + O_{2(g)} \rightarrow H_2O_{(s)}, \quad \Delta H = -241.8 \text{ kJ/mol.}$$
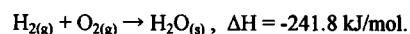
This principle can be used for generation of electricity and power. If MgO can be reduced back to magnesium again, a sustainable energy cycle would be established. For this process, the temperature of at least 4000 K is needed. Laser radiation is favorable for this purpose compared to direct solar radiation because of its high brightness that provides high enough intensity to achieve such temperature. Authors propose to convert solar radiation into laser radiation to realize reduction of Mg by solar power. The principle of laser reducing process resembles the thermal reduction process that is well-developed method known as Pidgeon method [1-4]. The solar-pumped laser using Fresnel lens as solar radiation collector was described as a cost-efficient converter, and feasibility of this proposed cycle as a robust and cost-effective fossil-fuel-free cycle was depicted [1, 5-7]. However, study of laser-induced magnesium reduction was conducted with common laser systems but not direct solar-pumped laser.

In this paper, demonstration of solar-pumped laser-induced magnesium production from MgO is described. A solar-pumped laser system suitable for magnesium energy cycle is proposed and designed here. Authors succeeded in producing magnesium from MgO by direct solar-pumped laser. A single beam 53 W solar-pumped laser is focused on a mixture of magnesium oxide with Si as reducing agent, corresponding to the deposition efficiency is 2.3 mg/kJ.
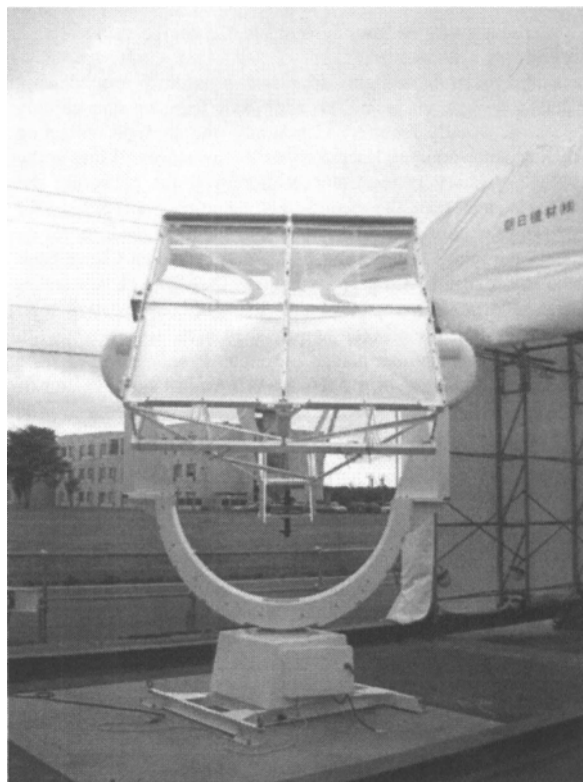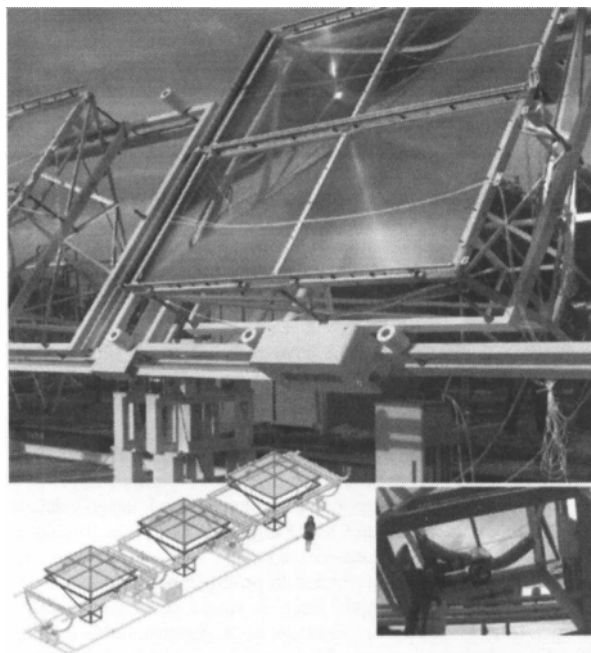

Fig. 1 Solar-pumped laser setup

Fig. 3 Solar-pumped laser setup a fundamental section of power plant

Fig. 2 Behavior of laser output for various laser rod shapes

Solar-pumped laser system for Mg energy cycle

Since the natural sunlight does not provide power density sufficient enough for lasing, an additional focusing and guiding devices are usually required. Commonly, the sunlight collecting system of solar-pumped laser consists of two stages. While at the fist-stage, primary concentrator is employed for collecting the sunlight to small spot, the second-stage pumping cavity is used for refocusing the collected solar power into the laser medium for an efficient pumping. A few solar-pumped laser systems have been previously realized with a mirror system [8-10]. Such researches have usually performed experiments using already existing solar facilities designed for other purposes such as solar towers. In order to construct power plants, a bundle of solar-pumped laser beams array scanning over MgO surface would be a section of energy renewal process in Mg cycle, therefore, the concentration devices must be flexible, inexpensive and not bulky.

Solar-pumped laser configuration

Laser output is able to be led to an MgO target using glass fiber and high intensity is realized by focusing techniques. In order dissociation of MgO in equilibrium, a temperature of 4000 K is needed because lower temperature may produce MgO vapor and reduce the deoxidization rate [2]. Such high temperature can be realized by an intensity of 10^5 W/cm^2 over MgO surface, therefore not only laser power but also its beam quality must be required.
Having these facts in mind, a large diameter Fresnel lens was adopted as an optical concentrator device for a new set up of solar pumped laser (Fig.1). Because of low weight, four-segmented Fresnel lens were assembled together to form a complete collector and mounted on a motor-driven bench, which is synchronized with sun trajectory in the sky. This system is one of the prototypes
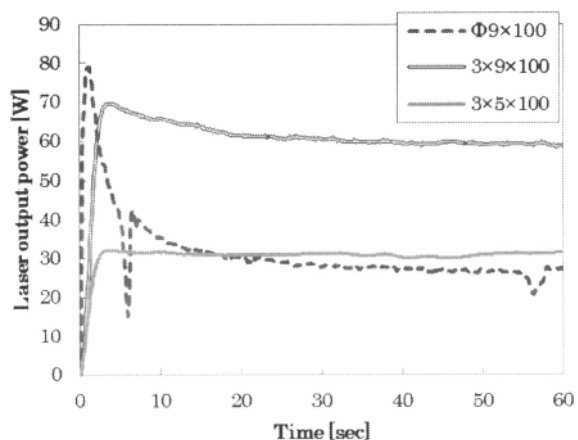
in a future solar-pumped laser plant (Fig. 2). All equipment including Fresnel lens and laser cavities follow sun trajectory automatically. Once the alignment of the laser cavity is achieved, a stable laser power is obtained while the system tracks the sun. As shown in Fig. 1, Fresnel lens (2×2 m^2, f=2 m) focuses the solar radiation toward laser cavities. Since the diameter of sun image at the focal point is limited to 20 mm, we used a conical cavity with input aperture diameter of 80 mm and cone angle of 20 deg (D80-θ20), the shape gave the best in the previous report [6, 7]. By a hybrid pumping scheme combining axial- and side-pumping configurations in which zigzag pumping light come from many directions along, a circular focal spot could be transformed for enhancing solar light absorption to a thin laser rod. Inner wall of pumping cavity is a cone-type mirror made of aluminum, which holds the laser medium along the central axis. One end of laser rod has high-reflection coating at the laser wavelength while the other end has antireflection coating.
Such solar-pumped laser system demonstrated its superiority by high output lasing. The maximum laser power of 80W was achieved with Nd^{3+}/Cr^{3+}:YAG rods of 9 mm in diameter and 100 mm in length (Φ9×100 mm) corresponding to total area performance (=laser output/Fresnel lens area) of 20 W/m2 which is 2.8 times larger than other previous works [10].

Feature of laser output

In order to realize a stable Mg production, laser output power must be stabilized. The behavior of laser output power for various laser rod shapes is shown in Fig. 3.
After reached a peak 80 W, laser output power of cylindrical Φ9×100 mm Nd^{3+}/Cr^{3+}:YAG rods decrease fast. Since the serious thermal effects along laser rod, stable out power is only about 30 W more than a factor of 2 below the maximum. Furthermore, the absorption is localized at the end of cone-shaped cavity and this leads to the break-up of laser media.
Laser output power is stabilized by using slab-shape laser rods because of their larger cooling surface. The maximum of stable output power of 60 W is achieved with a slab 3×9×100 mm Nd^{3+}/Cr^{3+}:YAG rod. However, the thermal effect along laser rod decreasing laser power is still observed here.

Proposal of high performance pumping and cooling cavity

In order to stabilize and improve the laser power, a uniform pumping and cooling effect along laser rod is needed. Authors here propose to use coolant inside a glass cooling blanket as a liquid light guide lens (LLGL) (Fig. 4(b)). The difference of refraction index between air and coolant is used to concentrate and guide pumping light to a thin active material (Fig. 4 (c)). The reflection power at the boundary, which did not penetrate inside the liquid lens, can be recollected by the secondary mirror, so low optical transfer loss is achieved. Furthermore, in liquid light-guide assembled system, lase material and cavity could be cooled separately so that more efficient cooling is realized. The higher flow velocities in cooling blanket leads to turbulent flow, leading to more efficient heat transfer process with a subsequent lower temperature drop.

Fig. 4 Calculation of absorption distribution along Nd^{3+}/Cr^{3+}:YAG and Nd:YAG laser rod with 14 mm-diameter of LLGL and without LLGL.

(a) Hybrid pumping cavity
(b) Hybrid pumping cavity with liquid light-guide lens

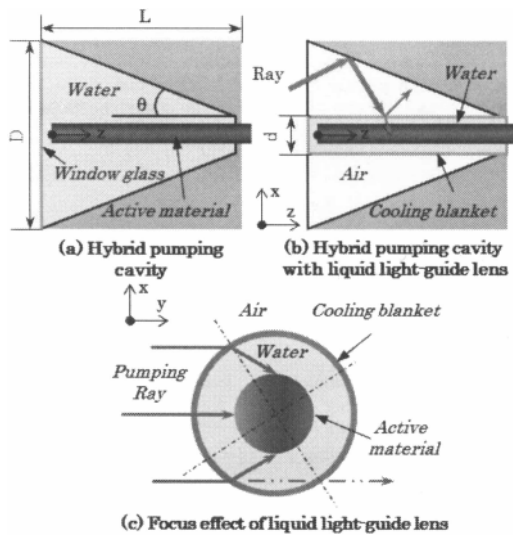(c) Focus effect of liquid light-guide lens

Fig. 5 (a) Cone-shape hybrid pumping cavity and (b), (c) liquid light guide lens configuration

The three-dimensional ray tracing has been performed to characterize the performance of LLGL. It includes:

1. Refraction, reflection, transmission at boundaries such as air-glass, glass-water, inner wall, Fresnel lens surface.
2. Absorption along each passage through various media including Fresnel lens material, water and laser material.

This ray tracing calculation was performed to simulate transmission through Fresnel lens of 2×2 m^2 area for all solar spectra considering the 4 mrad divergence angle of natural solar radiation. Absorption coefficient from 280 to 870 nm of Nd^{3+}/Cr^{3+}:YAG (Nd: 1.0, Cr: 0.1 at.%) was measured by Spectrophotometer (Jasco-V-530). Standard solar spectra of one and half air mass (AM1.5G) [11] and absorption coefficient of water in [12] are used as reference data.

Numerical results with slab 3×9×100 mm Nd^{3+}/Cr^{3+}:YAG show that the adopt of LLGL in hybrid pumping cavity leads to the increase of the total absorption power in laser material and reduces the strongly localized distribution of absorption power
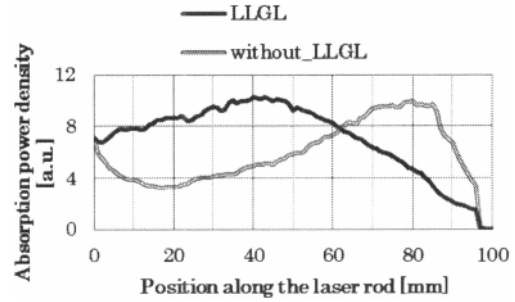
density along the rod as in Fig. 5. Because the LLGL enhances the refocusing sunlight by the air-liquid interface, the absorption at the input aperture increases, subsequently absorption peak at around 60-100 mm from the input aperture, that may lead to thermal damage because of high temperature drop on laser rod in the case without LLGL, is moderated. Therefore, high performance of pumping and cooling is achieved and a stable laser output of over 100 W is expected. Implementation of LLGL will be done in near future.

Experiments of solar-pumped laser-induce Magnesium reduction using reducing agent silicon

Experimental setup

The experimental setup is shown in Fig. 6. Here a chamber was used with the pressure of 7 Pa. The targets were prepared by mixing pure MgO powder and silicon powder, as follows:

1. Mixing magnesium oxide and silicon with molar ratio of 1: 0.5.
2. The mixture is packed into a cylindrical container that has diameter of 35 mm and height of 50 mm.
3. Compressing the target with a static pressure of 20 MPa to minimize the ejection of powder particles during laser irradiation.
4. Annealing the target at 110 °C for 3 hours to remove some of the gases absorbed in the mixtures.

The target was placed in the vacuum chamber. The cw solar-pumped laser of a slab 3×9×100 mm Nd^{3+}/Cr^{3+}:YAG rod irradiates vertically the target. Its beam qualities in the thickness direction M^2_t and in the width direction M^2_w are 60 and 193, respectively. Laser is focused by a condensing lens whose focus length is 40 mm. The laser spot side of 0.22×0.5 mm is calculated. The generated magnesium vapor was collected by a horizontally placed copper plate, forming a solid deposit. The mass of deposited material on the copper plate was measured, and the dipped into hydrochloric acid solution (HCl: 1 mol/l) as shown in Fig. 6. The following reactions are expected to take place:
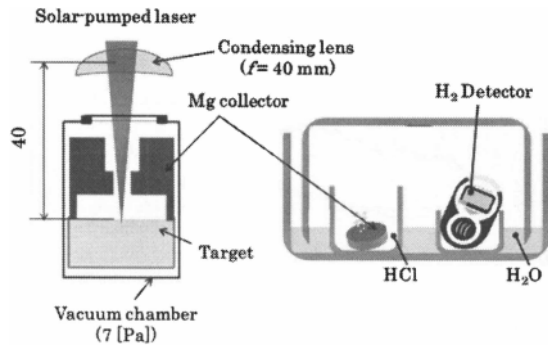
$$Mg_{(s)} + 2HCl_{(aq)} \rightarrow MgCl_{2(aq)} + H_{2(g)}$$

$$MgO_{(s)} + 2HCl_{(aq)} \rightarrow MgCl_{2(aq)} + H_2O_{(g)}$$
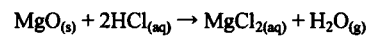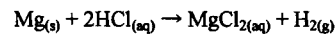
Fig. 6 Schematic of experimental set up and the hydrogen detector system.

Mg only among the deposited materials can produce hydrogen gas. The mount of emitted hydrogen gas was measured by the miniMAX XP hydrogen gas detector manufactured by Lumidor, which detects hydrogen gas in the range of 1-999 ppm (ml/m³). The generated hydrogen gas was accumulated in a water-sealed 1.6-l container. The amount of detected hydrogen was used to calculate magnesium mass, and the deposition efficiency (reduced Mg mass/ input laser energy).

Experiment and result

As results shown in Fig. 7, we have demonstrated successfully solar-pumped laser-induced magnesium reduction from MgO by using reducing agent silicon. At 50 W class of input laser power, the target was kept standstill and the laser duration time t was changed. The deposition efficiency of 2.3 mg/kJ was achieved when laser power, calculated laser intensity and laser duration were 53 W, 4.8×10^4 W/cm² and 5sec, respectively, since the laser power was too low and laser spot was too small compared with previous experiment. Such small spot might increase heat loss and so on. The deposition efficiency can be improved by higher input laser intensity. In previous report the deposition efficiency of 12.1 mg/kgJ had been achieved with laser intensity of about 10^5 W/cm² and mixing molar ratio of MgO:Si of 1:0.3 [3]. This laser intensity will be satisfied by the high efficient solar-pumped laser system which was proposed in previous section. Furthermore, the other conditions such as laser duration, mixing ratio must be optimized also for an efficient reduction.

Conclusion

It is important to note that the first time magnesium was produced by direct solar-pumped laser. We here have combined basis studies of laser-induced Mg reduction with solar-pumped laser technology. A solar-pumped laser system suitable for magnesium energy cycle was described. For stabilizing the laser output, slab laser rods was adopted, and high performance pumping and cooling cavity using LLGL was proposed. A single beam 55W solar-pumped laser whose beam qualities in the thickness direction M^2_t and in the width direction M^2_w are 60 and 193, respectively, was focused on a mixture of magnesium oxide with reducing agent silicon. The deposition efficiency of 2.3 mg/kJ was measured. In future study, implementation of solar-pumped laser with LLGL will be done and, focusing techniques of laser array for solar-pumped laser-induced magnesium production will be developed.
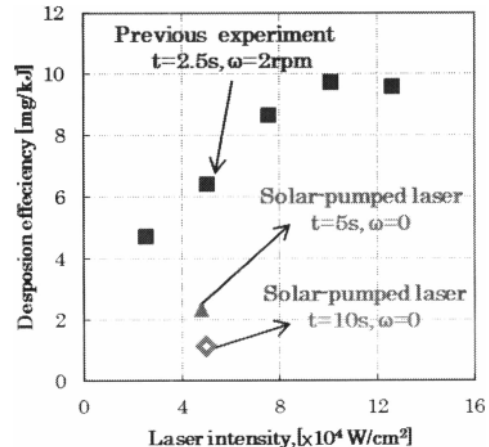

Fig. 7 Solar-pumped laser-induced magnesium reduction in compare with previous result [4]. MgO and Si were mixed with molar ratio of 1: 0.5. t and ω are the laser duration time and target rotation speed, respectively.

Reference

1. T. Yabe, S. Uchida, K. Ikuta, K. Yoshida, C. Baasandash, M. S. Mohamed, Y. Sakurai, Y. Ogata, M. Tuji, Y. Mori, Y. Satoh, T. Ohkubo, M. Murahara, A. Ikesue, M. Nakatsuka, T. Saiki, S. Motokoshi, and C. Yamanaka, Appl. Phys. Lett. 89, 261107 (2006).
2. T. Yabe, M. S. Mohamed, S. Uchida, C. Baasandash, Y. Sato, M. Tsuji, and Y. Mori J. Appl. Phys. 101, 123106 (2007)
3. M. S. Mohamed, T. Yabe, C. Baasandash, Y. Sato, Y. Mori, Liao Shi-Hua, H. Sato and S. Uchida, J. Appl. Phys. 104, 113110 (2007).
4. S. H. Liao, T. Yabe, M. S. Mohamed, C. Baasandash, Y. Sato, C. Fukushima, M. Ichikawa, M. Nakatsuka, S. Uchida, and T. Ohkubo, J. Appl. Phys. 109, 013103 (2011).
5. T. Yabe, T. Ohkubo, S. Uchida, K. Yoshida, M. Nakatsuka, T. Funatsu, A. Mabuti, A. Oyama, K. Nakagawa, T. Oishi, K. Daito, B. Bagheri, Y. Nakayama, M. Yoshida, S. Motokoshi, Y. Sato, and C. Baasandash, Appl. Phys. Lett. 90, 261120 (2007).
6. T. Ohkubo, T. Yabe, K. Yoshida, S. Uchida, T. Funatsu, B. Bagheri, T. Oishi, K. Daito, M. Ishioka, Y. Nakayama, N. Yasunaga, K. Kido, Y. Sato, C. Baasandash, K. Kato, K. Yanagitani, and Y. Okamoto, Opt. Lett. 34(2) (2009).
7. T. Yabe, B. Bagheri, T. Ohkubo, S. Uchida, K. Yoshida, T. Funatsu, T. Oishi, K. Daito, M. Ishioka, N. Yasunaga, Y. Sato, C. Baasandash, Y. Okamoto, and K. Yanagitani, J. Appl. Phys. 104, 083104 (2008).
8. C. G. Young, Appl. Opt. 5, 993 (1966).
9. V. Krupkin, Y. Kagan, and A. Yogev, Proc. SPIE 2016, 50 (1993).
10. M. Lando, J. Kagana, B. Linyekina, and V. Dobrusin, Opt. Commun. 222, 371 (2003).
11. ASTM International, ASTM G173-03 Reference Spectra Derived from SMARTS v. 2.9.2 (2004).
12. G. M. Hale and M. R. Querry, Appl. Opt. 12(3), 555 (1973).